OPEN ACCESS
Journal of Multidisciplinary Applied Natural Science Vol. 6 No. 2 (2026) https://doi.org/10.47352/jmans.2774-3047.379
Check for updates
Research Article

Beyond Waste: Unlocking the Potential of Cassava By-products for Biomedical Hydrogels with Effective Drug Delivery Capabilities

Heri Satria*, Kamisah Delilawati Pandiangan, Hapin Afriyani, and Diska Indah Alista

Received : August 11, 2025	Revised : March 6, 2026	Accepted : March 11, 2026	Online : April 18, 2026

Abstract
A substantial number of by-products, such as peel and residue, are generated from cassava production in Indonesia but are often neglected, posing a significant environmental challenge. In response to this issue, this research reports the valorization of these processing by-products into functional, cellulose-based hydrogels for drug delivery applications. The research developed an optimized methodology that ensures the near-complete removal of starch from cassava-based waste. This process consistently yields isolated cellulose characterized by a dual-population size distribution across both waste sources, reflecting the successful extraction of distinct fiber fractions. The synthesis of these hydrogels via graft polymerization was supported by Fourier transform infrared (FTIR) analysis, which showed the emergence of characteristic peaks for C=O and N–H groups indicated the incorporation of the graft polymer into the hydrogel network. The results revealed notable structural and performance differences, with the cassava residue cellulose (CRC)-hydrogel exhibiting a superior, highly porous, and well-interconnected network compared with cassava peel cellulose (CPC)-hydrogel. This translated to a greater maximum swelling ratio (51.87 g/g) and enhanced water retention, which directly influenced its drug delivery capabilities. The CRC-hydrogel demonstrated a higher entrapment efficiency for ascorbic acid (22.47 w/w%) and a faster, more predictable diffusion-controlled release profile, as confirmed by Higuchi kinetic modelling. Furthermore, it proved to be a more effective delivery system for amoxicillin at a concentration of 25 µg. This study concludes with a systematic route for the fabrication of value-added functional hydrogels from abundant agricultural waste. This work helps in sustaining the environment and utilization of biocompatible material for biomedical applications (drug delivery, wound healing) by providing a reliable synthetic path from cassava residue to porous matrix.

Keywords: cassava peel, cassava residue, cellulose, drug delivery, graft polymerization, hydrogel

1. INTRODUCTION

High cassava production in Indonesia, particularly in Lampung Province, which contributed nearly 40% of the national output in 2022, generates a massive amount of lignocellulosic waste [1][2]. These residues are often discarded, resulting in environmental problems such as odor pollution and land contamination [3][4]. The global production of this commodity has reached approximately 302 million tonnes, and it was notable that approximately 25-30% w/w is discarded as fibrous residue and peels [5]. However, in line with the global push for a circular economy, there's a growing interest in repurposing this agricultural waste, which is rich in cellulose. Studies show that the residues are excellent sources of cellulose, with content in peels ranging from 39.78% to 66.00% [2][6]-[8]. This abundant biomass presents a compelling opportunity for valorization by converting waste into high-value materials [9][10].

Amongst, the most promising applications is the development of cellulose-based hydrogels [11]. Hydrogels are three-dimensional polymeric networks that can absorb and retain large amounts of water, making them highly versatile. By grafting monomers like acrylamide onto the cellulose backbone, researchers can create hydrogels with enhanced properties, such as improved swelling and mechanical strength [12][13]. This modification enables precise control over the hydrogel's characteristics, allowing them to be tailored for specific functional requirements. This innovative approach not only addresses environmental concerns but also offers significant benefits for the biomedical sector [14]-[16].

A significant gap in waste valorization needs to be addressed. Recent advancements in biomaterials have led to a surge in cassava-based hydrogel research, with studies exploring starch-based

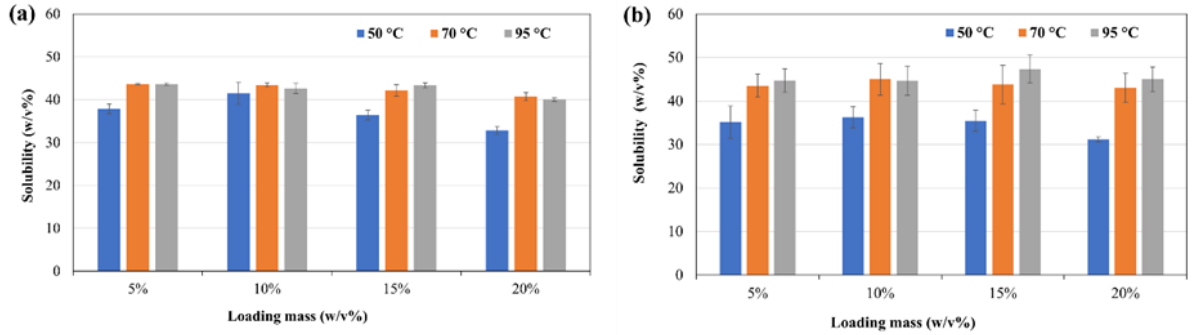

Figure 1. Effect of temperature and loading mass on the solubility of (a) cassava peel powder and (b) cassava residue powder.

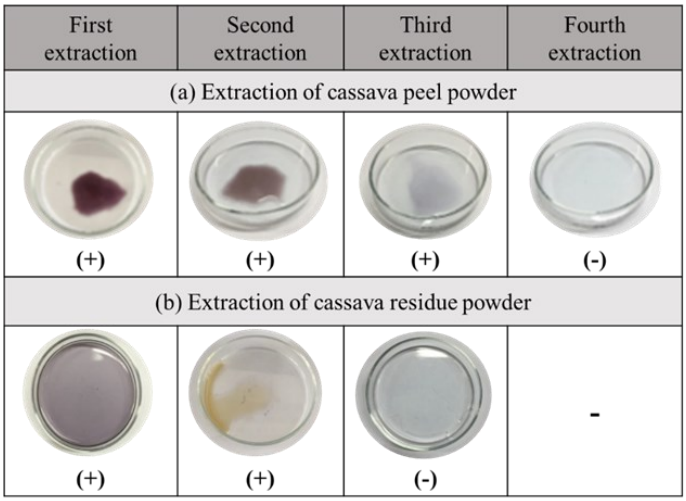

Figure 2. Results of the iodine test for starch removal from (a) cassava peel powder and (b) cassava residue powder. The (+) symbol indicates a positive test for starch, while the (-) symbol indicates a negative test, signifying complete removal of starch.

matrices [17][18] and composite systems for environmental or medical use [19][20]. However, a majority of these studies utilize the starch component or commercially available cellulose derivatives. While various cellulose sources have been explored, the differential impact of using specific cassava processing byproducts as starting feedstocks has not been sufficiently explored for the extraction purpose. Pointedly, there is a lack of entire research that integrates the entire process from initial waste treatment to the final evaluation of the hydrogel as a drug delivery system. Chemical modifications, such as the application of sonication and the addition of specific functional groups, have been shown to enhance hydrogel properties for medical use, but these processes have yet to be fully integrated into a complete and optimized workflow for cassava waste [21][22].

This research presents an innovative and improved approach, precisely detailing each stage of the process. We will achieve this through four key steps: first, by optimizing the starch removal from cassava waste; second, by isolating the cellulose; third, by producing ingenious hydrogels via the grafting of acrylamide; and finally, by evaluating their practical utility as a controlled drug delivery system for ascorbic acid and amoxicillin. This approach, which connects local waste valorization with a specific and practical biomedical application, is designed to contribute to both environmental sustainability and healthcare innovation within a circular economic framework.

2. MATERIALS AND METHODS

2.1. Materials

The cassava roots used in this study were sourced from Lampung Tengah, Indonesia. Cassava

peels and residue were obtained as byproducts during the starch extraction process from cassava tubers. The chemicals, i.e., iodine, H_2SO_4, KOH, ammonium persulfate (APS), acrylamide (Aam), *N*,*N*′-methylenebisacrylamide (MBA), KI, KIO_3, ascorbic acid (AA), Muller-Hinton Agar (MHA) were analytical grade and purchased by Merck, respectively; since amoxicillin trihydrate (Hexpharm) was obtained from commercial medicine. *Staphylococcus aureus* ATCC 25923 was obtained from the Indonesian Culture Collection, National Research and Innovation Agency (BRIN).

2.2. Methods

2.2.1. Cassava Peel and Residue Preparation

Cassava roots were cleaned, sanitized, and peeled by hand. The pulp was then sectioned, weighed, and pulverized with a blender. Starch was extracted from the pulp using the wet milling method [23]. The byproduct, peelings and residue, were dried in a forced-air oven at 60 °C for 24 h. They were then crushed in hammer mills and sieved through a 120-mesh screen to create microparticles. These microparticles were stored in sealed containers until cellulose isolation.

2.2.2. Starch Removal from Cassava Peel and Residue Flour

Starch was removed from cassava peel and residue flour by testing various flour mass loadings (5, 10, 15, and 20%) at different temperatures (50, 70, and 95 °C). For each trial, the flour was added to an Erlenmeyer flask with 100 mL of distilled water. This mixture was then heated at the target temperature for 10 min before being cooled to room temperature. After cooling, the mixture was centrifuged to separate the filtrate from the sediment. The resulting precipitate was then used for the cellulose extraction process from the cassava peel and residue. To determine the optimum conditions for starch removal, the collected data were analyzed using a two-way ANOVA, followed by Tukey's HSD as a post hoc test. The extraction process was repeated until the iodine test yielded no purple coloration in the filtrate, indicating that the starch had been completely removed.

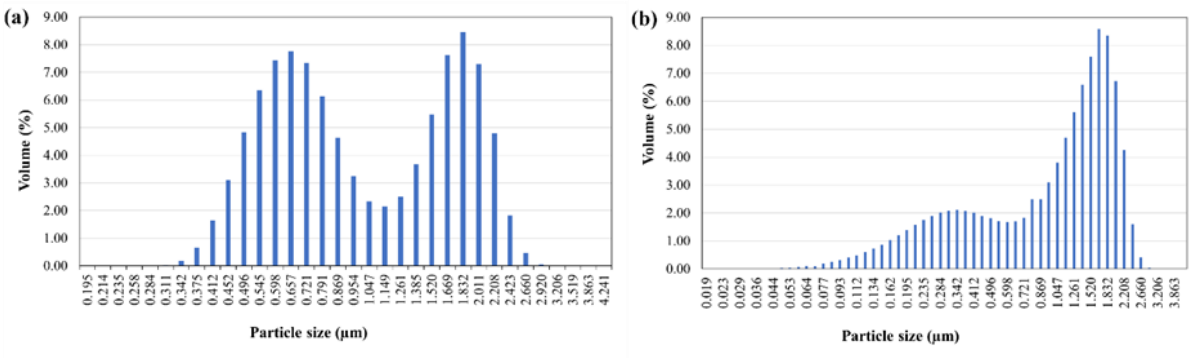

Figure 3. Particle size distribution of isolated cellulose from (a) CPC, and (b) CRC, showing a dual-distribution particle size characteristic for both materials.

Figure 4. Photographs of the synthesized dried cellulose-based hydrogels: (a) CPC-hydrogel from CPC, and (b) CRC-hydrogel from CRC.

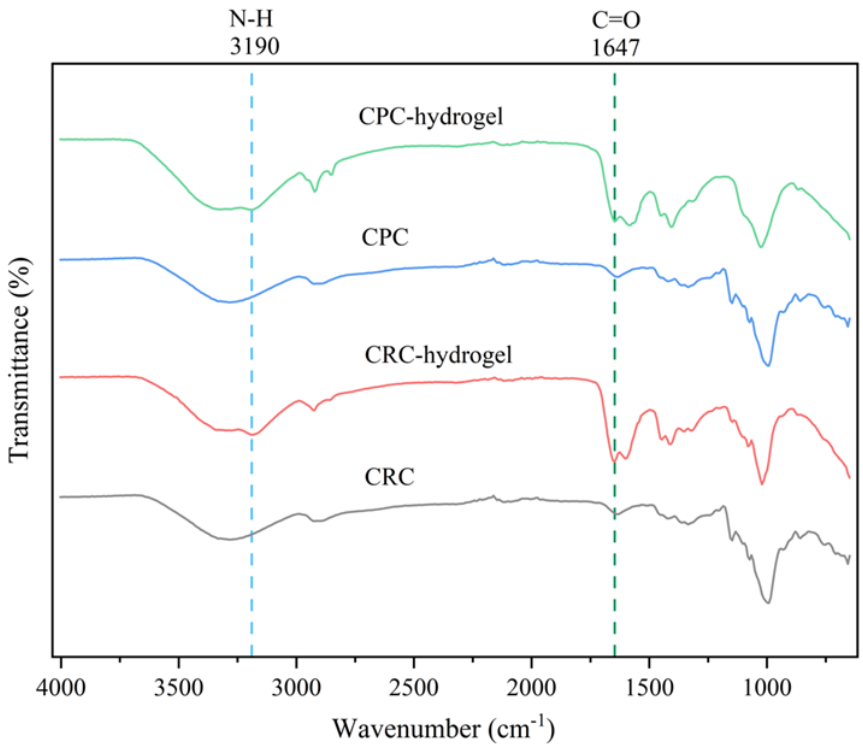

Figure 5. In comparison to the source of cellulose (CPC and CRC), the FTIR spectra of CPC-hydrogel and CRC-hydrogel provide evidence of successful polymerization.

2.2.3. Acidic Treatment and Mechanical Size Reduction

Cellulose powder (10% w/v) was dissolved in 0.5 M H_2SO_4 and homogenized at 40–60 °C for 1 h [24]. After neutralizing the mixture with 5% (w/v) KOH to a neutral pH, the resulting precipitate was suspended in distilled water to form a 5% (w/v) suspension. This suspension was then sonicated at 40 kHz for 1h. The mixture was centrifuged at 10,000 rpm for 10 min, and the resulting sediment was dried using a vacuum freeze dryer. Finally, the particle size of the product was characterized using a Beckman Coulter LS 13 320 Particle Size Analyzer.

2.2.4. Synthesis Procedure of Hydrogels

To synthesize the hydrogels, 1 g of dry cellulose was first made into a pulp with distilled water and heated to 95 °C for 30 min. After cooling to 60 °C, 0.05 g of APS was added and stirred for 15 min. Next, a solution containing 5 g of AAm and 5 mg of MBA in 40 mL of distilled water was added. The temperature was then increased to 70 °C and maintained for 3 h. The final product was precipitated using an ethanol/methanol mixture, purified by refluxing with acetone for 1 h, and then characterized using an Agilent FTIR.

2.2.5 Evaluation of Swelling Ratio and Water Retention

The swelling and water retention of the hydrogels were measured using gravimetric analysis. To determine swelling capacity, a precisely weighed, dried hydrogel was immersed in 50 mL of deionized water. At specific time points, the swollen hydrogel was removed, blotted to remove surface water, and weighed using an analytical balance. To measure water retention, the equilibrated hydrogel was left at ambient temperature, with its weight monitored at regular intervals until it stabilized. The swelling ratio and percentage of water retention were then calculated using Equations 1 and 2, respectively;

$$Swelling\ ratio(Sg/g) = \frac{W - W_0}{W_0} \quad \textbf{(1)}$$

$$Water\ retention\ (\%) = \frac{W_t - W_0}{W_d - W_0} \times 100\% \quad \textbf{(2)}$$

where W_t is the swollen hydrogel weight at time intervals, W_o is the weight of the dried hydrogel,

and W_d is the initial weight of the swollen hydrogel.

2.2.6. Evaluation of AA Absorption and Release

The capacity of the hydrogel to absorb and release AA was evaluated through a series of experi ments. For absorption, 0.1 g of dry hydrogel was immersed in 25 mL of a 100 mg/L AA solution for up to 48 h. The loaded hydrogels were then immersed in 25 mL of distilled water for 72 h to assess the release of AA. The concentration of released AA was quantified via iodometric titration, where 1 mL of 0.002 M KIO_3 solution was equivalent to 0.8806 mg of AA ($C_6H_8O_6$). For a more detailed release profile, AA concentration was measured at intervals up to 24 h. The Higuchi kinetic model was then applied to analyze the release kinetics by plotting the cumulative AA release percentage against the square root of time.

2.2.7. Evaluation of Antibiotic Release

The capacity of the hydrogel to release antibiotics was assessed using a modified Kirby-Bauer disk diffusion assay. To prepare, 0.1 g of dry hydrogel were soaked for 24 h in 1 mL of diluted amoxicillin solutions at various concentrations (0, 25, and 50 µg). The resulting amoxicillin-loaded, swollen hydrogel was then placed onto MHA that had been swabbed with 24-h cultures of *S. aureus*.

3. RESULTS AND DISCUSSIONS

3.1. Starch Removal and Solubility Analysis of Cassava Waste

The process of removing starch from cassava peel and residue powder was thoroughly investigated by examining how solubility changed with temperature and mass. As shown in Figure 1, temperature is the most influential factor. As the temperature rose from 50 to 95 °C, solubility consistently increased because thermal energy broke down starch granules, allowing them to dissolve in water. The solubility of cassava starch is intricately linked to this thermal treatment, where heating below 100 °C disrupts hydrogen bonds, causing starch granules to swell and increase in solubility [25]. Interestingly, cassava residue powder always showed higher solubility than cassava peel powder, which suggests that its starch might be more accessible due to a simpler cell wall structure. This initial analysis helped identify the

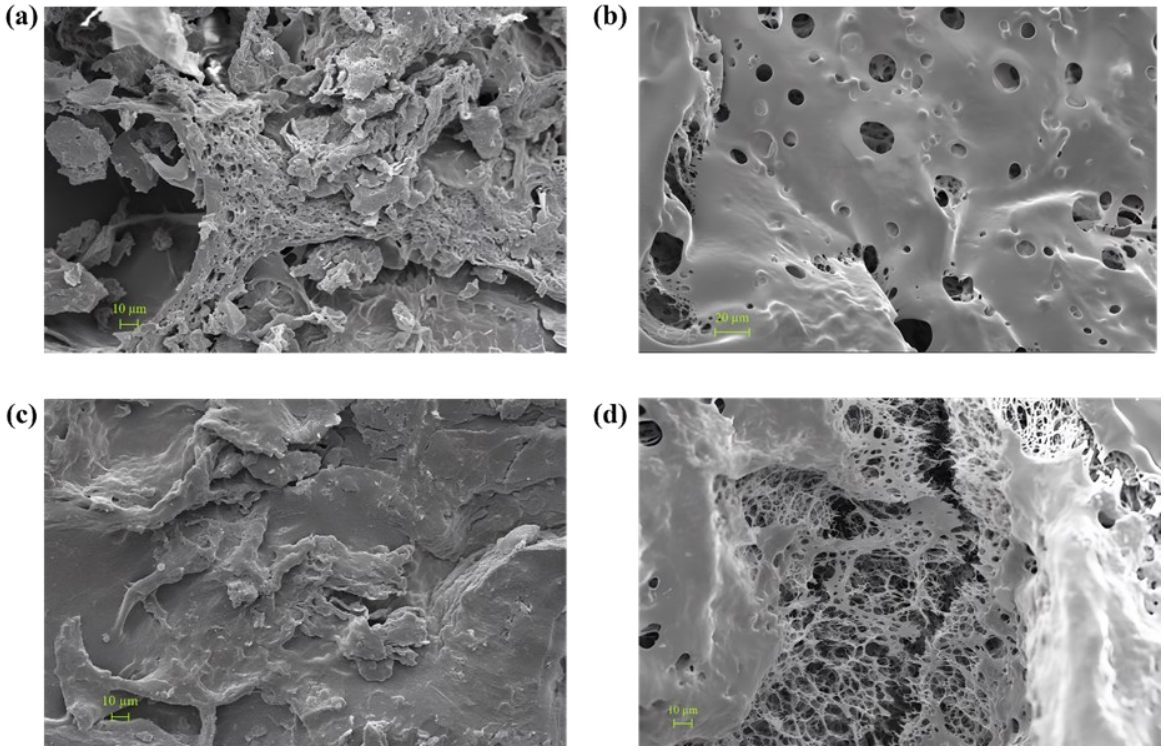

Figure 6. SEM micrographs showing the morphology of the hydrogels: (a) dried CPC-hydrogel, (b) swollen CPC-hydrogel, (c) dried CRC-hydrogel, and (d) swollen CRC-hydrogel.

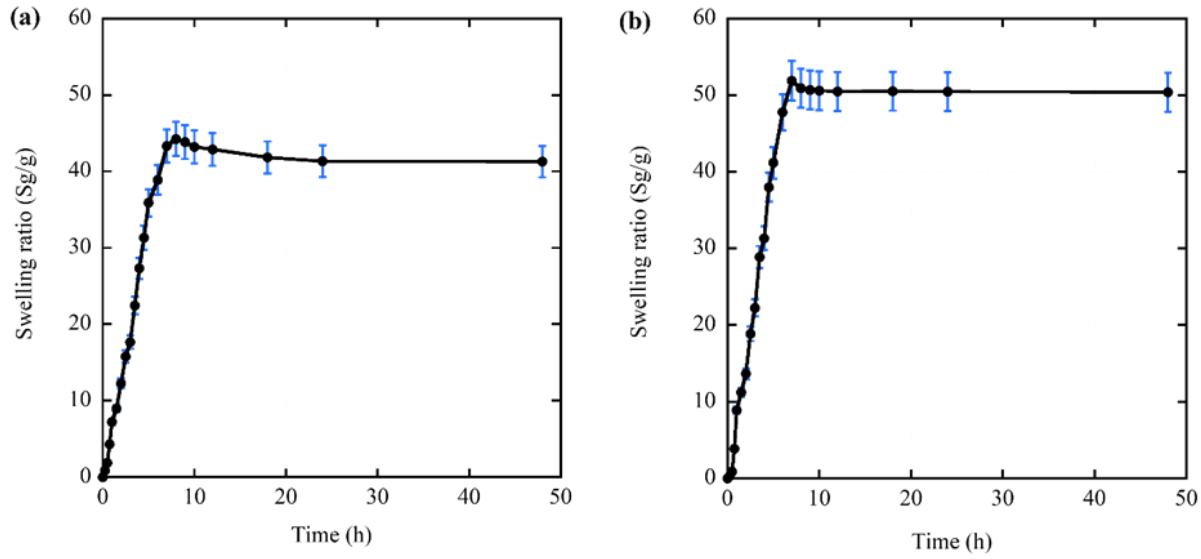

Figure 7. Swelling kinetics of the synthesized hydrogels: (a) CPC-hydrogel, and (b) CRC-hydrogel.

key variables affecting the extraction process.

A detailed statistical analysis was performed to find the best conditions for starch removal. Statistical analysis via two-way ANOVA revealed that while temperature exerted a significant influence on solubility ($p < 0.001$), on the other hand, the loading mass did not act as a critical determinant within the tested range ($p = 0.337$). Although a slight numerical decrease in solubility was observed at the highest mass concentrations, this trend was not statistically significant. The Post Hoc tests indicate that the solubility at 70 °C was the optimal temperature. While the highest solubility at 95 °C was not practical for separating the starch from the cellulose because it tends to create a gelatinous mass, which increases the viscosity [26].

Based on our findings, the best conditions for removing starch were a loading mass of 10 w/v% at 70 °C. Under these conditions, cassava peel and cassava residue flours showed high solubilities of 43.43 and 45.01 w/v%, respectively, while avoiding the formation of a gelatinous mass. To confirm that all starch was removed, an Iodine test was performed. A clear solution indicated that the extraction was complete. As shown in Figure 2, cassava peel flour needed four extractions, while cassava residue flour only needed three. This difference likely comes from the natural variations in their starch solubility and structure.

3.2. Particle Size Analysis of Isolated Cellulose

Particle size analysis of the cellulose from both cassava peel (CPC) and cassava residue (CRC) showed a consistent dual-distribution particle size distribution, meaning each sample had two distinct particle groups. As seen in Figures 3(a) and 3(b), the average particle sizes were very similar: 1.214 ± 0.692 µm for CPC and 1.190 ± 0.698 µm for CRC. The CPC had two main peaks at approximately 0.6 and 1.8 µm, while the CRC had its peaks at about 0.35 and 1.7 µm. The close similarity in these distributions and the nearly identical mean and median values (0.952 µm for CPC vs. 0.948 µm for CRC) suggest that our processing method produced cellulose with highly similar size characteristics, even though the original raw materials likely had different fibrous structures.

Cellulose derived from biomass like cassava peels has a diverse particle size range, which can exhibit different behaviours when subjected to various mechanical treatments such as sonication. Studies have shown that sonication can fragment larger cellulose aggregates into nanosized particles, resulting in a dual-distribution particle size [27] indicated that manipulating particle size during the preparation of cellulose nanofibers could yield this type of particle size distribution, which in turn impacts the material's mechanical properties and performance. This finding is further supported by Hachaichi et al. [28], who explained that morphological changes in cellulose during

mechanical processing contribute to the formation of distinct size classes within the particle distribution. Their observations of needle-like particles suggest that mechanical treatments applied to cassava cellulose could result in particle morphologies with distinct peaks, leading to a heterogeneous particle size distribution.

3.3. Hydrogel Formation and Characterization

The synthesis of cellulose-based hydrogels from both CPC and CRC was successfully carried out through a graft polymerization process. The procedure involved creating a cellulose pulp, followed by the addition of APS as a free radical initiator, which led to the formation of active sites on the cellulose backbone. Subsequently, the monomers of Aam and the cross-linking agent MBA were introduced. The polymerization was initiated at 70 °C, a temperature carefully chosen to promote the grafting reaction without degrading the cellulose structure. The final products, depicted in Figure 4, show the resulting hydrogels in a dried state after precipitation and purification. Visually, both samples appear as solid, granular materials, indicating successful cross-linking and formation of a three-dimensional polymer network. The darker color of the hydrogel from CPC in Figure 4(a) is likely due to the inherent color of the raw cassava peel itself, whereas the lighter color of the hydrogel from CRC in Figure 4(b) reflects the original, lighter shade of the cassava residue flour.

3.4. Confirmation of Grafting and Cross-linking by FTIR Spectroscopy

The FTIR analysis was applied to confirm that grafting and cross-linking were successful in both the CPC-hydrogel and CRC-hydrogel. As shown in Figure 5, the spectra of the hydrogels displayed new peaks for the C=O and N-H functional groups clearly, which were completely absent in pure cellulose. These new peaks serve as direct evidence of the successful copolymerization reaction [29].

Specifically, the CPC-hydrogel showed a C=O peak at 1647 cm^{-1} and an N-H peak at 3190 cm^{-1}. Similarly, the CRC-hydrogel exhibited a C=O peak at 1654 cm^{-1} and an N-H peak at 3190 cm^{-1}. The consistent appearance of these two key peaks confirms that the acrylamide monomer was successfully grafted onto the cellulose backbone in both materials, leading to the formation of the hydrogel network [12][30][31].

FTIR spectroscopy is an essential tool for understanding the chemical structure and intermolecular interactions within these hydrogels. The analysis reveals key spectral features, such as the O–H stretching vibrations around 3400–3500 cm^{-1}, which are linked to successful hydrogel formation. Other bands, like the C–H stretching around 2870 cm^{-1} [32], also confirm successful interaction between the cellulose and acrylamide chains. This comprehensive analysis allows for a clearer understanding of the chemical interactions that lead to improved properties like enhanced swelling and mechanical strength [33].

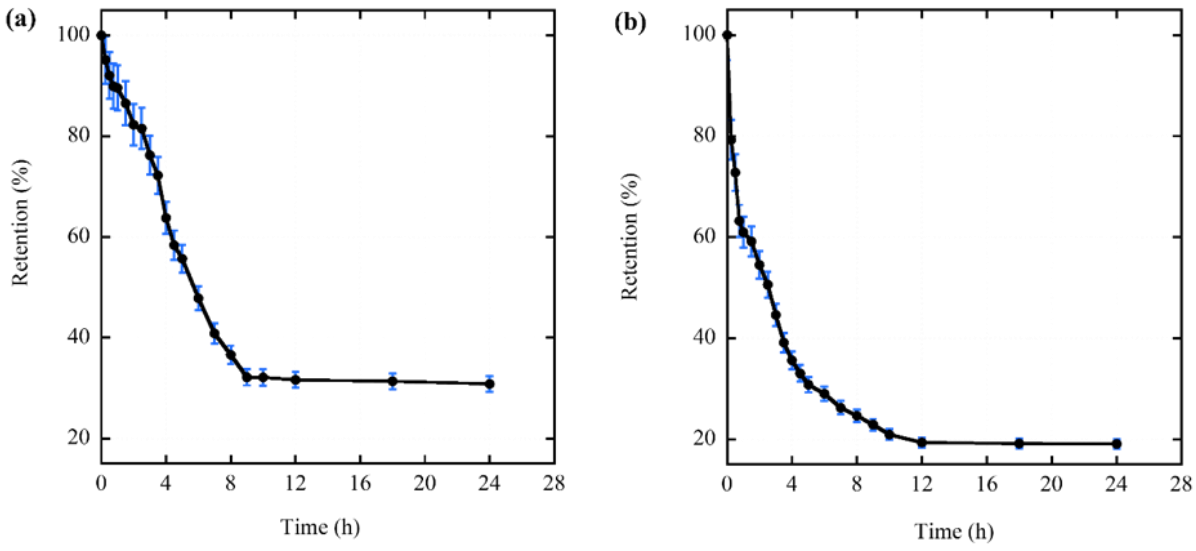

Figure 8. Water retention kinetics of the synthesized hydrogels: (a) CPC-hydrogel, and (b) CRC-hydrogel.

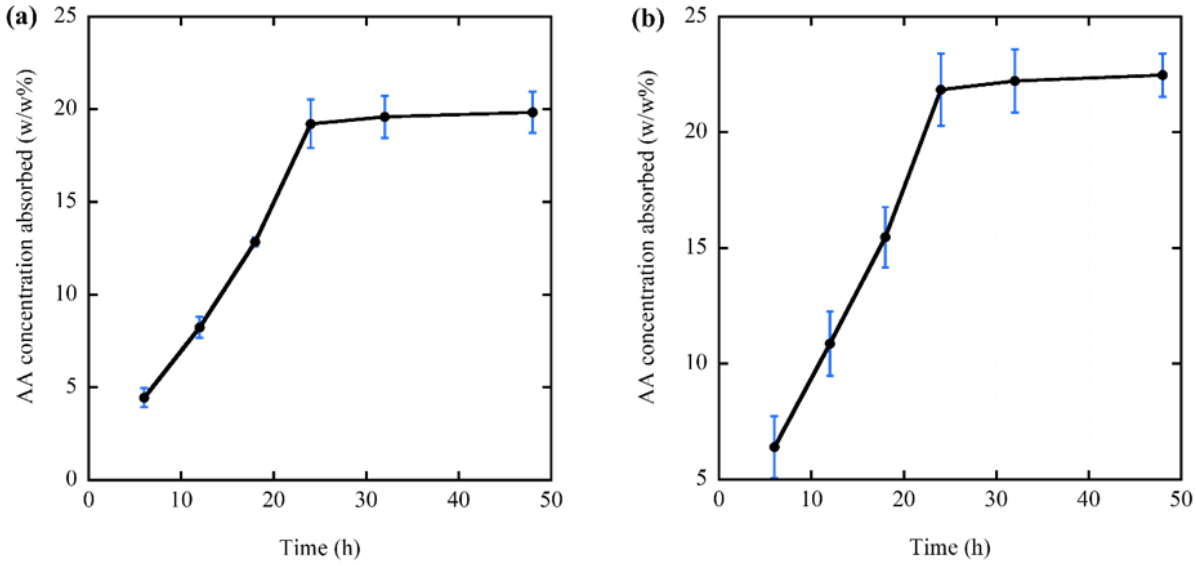

Figure 9. Entrapment kinetics of ascorbic acid by (a) CPC hydrogel and (b) CRC hydrogel.

Furthermore, FTIR spectrum helps reveal the effective formation of a stable polymeric network [34] and aids in optimizing hydrogel formulations by showing chemical shifts associated with varying degrees of acrylamide incorporation and crosslinking ratios [35].

3.5. SEM Analysis of Hydrogel Morphology

SEM studied the structural morphology of the hydrogels to correlate it with their functional properties. As shown in Figure 6, the dried CPC-hydrogel and CRC-hydrogel both have relatively dense, solid structures, which confirms the formation of a cross-linked polymer matrix. However, significant differences appear once the hydrogels swell. The swollen CRC-hydrogel in Figure 6(d) displays a highly porous, three-dimensional network with well-defined, interconnected pores. This open structure directly explains its superior performance, as a more open network allows for greater water absorption and more efficient retention. In contrast, the swollen CPC-hydrogel in Figure 6(b) has smaller, more irregular pores and a less interconnected network. This difference in pore morphology directly accounts for its lower swelling ratio and water retention capacity. Ultimately, the superior porous structure of the CRC-hydrogel is a key factor in its more effective performance for drug and antibiotic delivery applications.

SEM analysis is a valuable tool for understanding the morphology of cellulose hydrogels, revealing a porous structure that is beneficial for drug delivery, as it allows for significant drug loading and efficient water absorption [36]. However, this morphology is not static; it is heavily influenced by the preparation methods [37] emphasized that varying processing techniques can alter the pore size and distribution, which are critical for optimizing drug release kinetics. Furthermore, the use of cross-linking agents, as reported earlier [38], causes specific structural modifications, such as tighter packing and reduced porosity. This not only influences swelling and drug retention but also enhances the hydrogel's mechanical strength for effective sustained-release applications.

3.6. Swelling Ratio and Retention

The swelling behavior of the synthesized hydrogels was evaluated to determine their water absorption capacity. As shown in Figure 7, both hydrogels exhibited a rapid initial swelling phase followed by a gradual increase until they reached an equilibrium state. This pattern confirms the successful formation of a cross-linked polymer network capable of absorbing and retaining a significant amount of water. A comparative analysis revealed that the CRC-hydrogel in Figure 7(b) demonstrated a significantly higher maximum swelling ratio. It reached a peak of 51.87 g/g at 7 h and maintained this high level, stabilizing at 50.38

g/g after 48 h. In contrast, the CPC-hydrogel in Figure 7(a) reached a lower peak of 44.23 g/g at 8 h and stabilized at a lower level of 41.28 g/g after 48 h. This difference can be attributed to the inherent structural and chemical properties of the cellulose from each source, such as crystallinity or particle size, which affect the efficiency of the grafting polymerization and the density of the resulting hydrogel network.

The water retention capacity of the hydrogels was also evaluated to understand their ability to retain water over time. As shown in Figure 8, both hydrogels showed a trend of rapid initial water loss that then stabilized at an equilibrium retention level. A comparison revealed a clear difference in their retention capabilities. The CPC-hydrogel in Figure 8(a) had superior long-term retention, with its water content stabilizing at 30.85% after 24 h. Conversely, the CRC-hydrogel in Figure 8(b) released over 50% of its water in the first 2.5 h, and its long-term retention was significantly lower, stabilizing at 19.11% after 24 h.

This difference in long-term retention capability can be attributed to a more stable or denser cross-linked structure in the CPC hydrogel. Cellulose-based hydrogels are recognized for these properties, which are critical for applications like drug delivery, as the incorporation of cellulose and nanocrystals can enhance water uptake speed and absorption capacity [39]. This structural integrity, which is influenced by factors like microcrystalline cellulose [40] and nanocrystals [41][42], is advantageous for encapsulating various drugs.

3.7. Absorption and Release of Vitamin C

The ability of the hydrogels to trap AA was evaluated as a key step for drug delivery. As shown in Figure 9, both hydrogels followed a similar pattern: a fast initial phase, a steady increase, and then a leveling off when they were full of AA. The CRC-hydrogel, in Figure 9(b), was much better at trapping AA than the CPC-hydrogel, in Figure 9(a). By 24 h, the CPC-hydrogel had trapped 19.21 w/w%, while the CRC-hydrogel reached a higher 21.84 w/w%. This superior performance by the CRC-hydrogel is directly linked to its better swelling and water retention capabilities. Its more porous structure allows for more AA molecules to diffuse in and be held within the network.

The release of AA from both hydrogels followed a two-stage profile, as shown in Figure 10. This profile is characterized by a rapid initial burst followed by a slower, more sustained release. The CPC-hydrogel, in Figure 10(a), showed a faster initial release, with 61.98% released within 6 h. In contrast, the CRC-hydrogel in Figure 10(b) had a slower initial rate but achieved a more sustained release over time. These differences in release kinetics are directly influenced by the hydrogel's structural properties, such as swelling, porosity, and cross-linking density [31][43]. The faster initial release from the CPC-hydrogel may be due to a

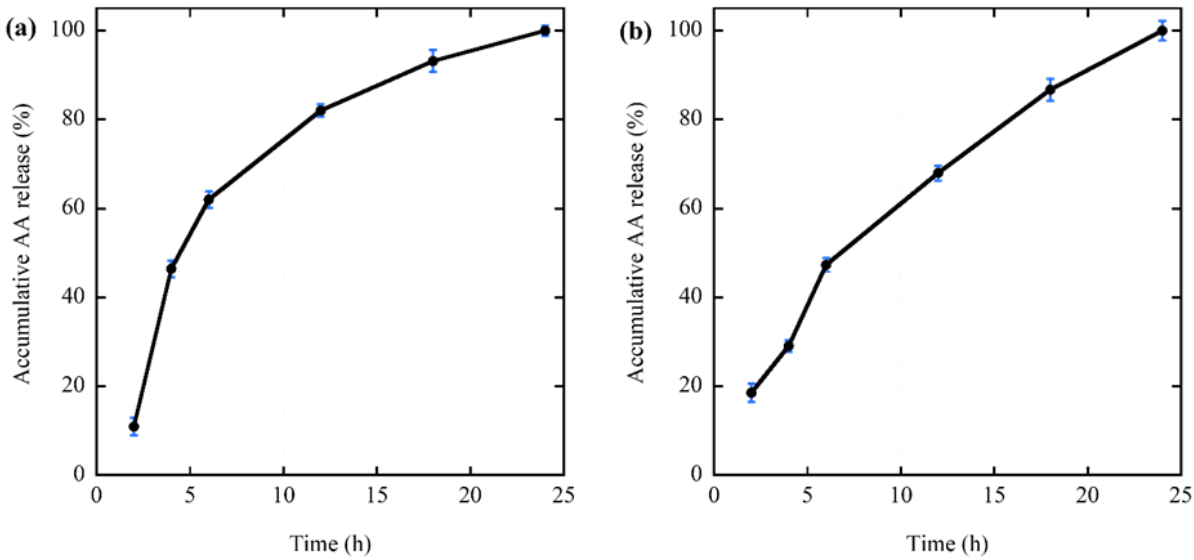

Figure 10. Accumulative release of ascorbic acid (AA) from (a) CPC-hydrogel and (b) CRC-hydrogel.

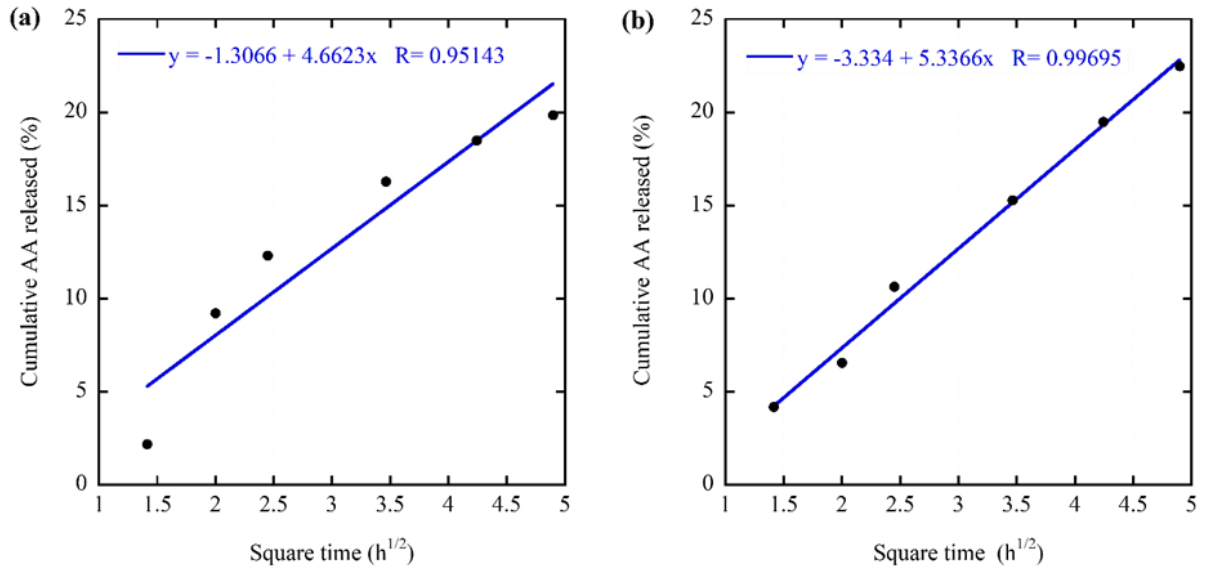

Figure 11. Higuchi kinetic plots for the release of ascorbic acid (AA) from (a) CPC-hydrogel and (b) CRC-hydrogel.

more open structure, while the CRC-hydrogel's behavior suggests a more complex release mechanism likely influenced by its denser polymer network, which is consistent with its high swelling capacity.

Analysis using the Higuchi kinetic model further confirmed that the release of AA from both hydrogels is a diffusion-controlled process. As seen in Figure 11, both hydrogels fit the model well, showing a strong linear relationship between cumulative release and the square root of time. The CRC-hydrogel, in Figure 11(b), exhibited a superior fit with an R-value of 0.99699 compared to the CPC -hydrogel with an R-value of 0.95143, in Figure 11 (a). This suggests that the diffusion mechanism of CRC-hydrogel is more predictable. The Higuchi constant (k), which represents the diffusion rate, was higher for the CRC-hydrogel (k = 5.3366) than for the CPC-hydrogel (k = 4.6623), indicating a faster diffusion rate. This finding is consistent with the CRC-hydrogel's more porous structure and superior swelling capacity. These results confirm that while both hydrogels release AA through diffusion, their different physical structures directly affect the release rate, which is a key factor for developing effective drug delivery systems [44]-[46].

3.8. Hydrogel Performance in Antibiotic Delivery

The effectiveness of the hydrogels as antibiotic delivery systems was evaluated using the Kirby-Bauer disk diffusion assay, with the results shown in Figure 12. The clear zones of inhibition around the hydrogel samples at 25 and 50 µg concentrations confirmed that both the CPC-hydrogel and CRC-hydrogel successfully absorbed and released amoxicillin. As expected, the size of the inhibition zone was concentration-dependent, with larger zones at higher antibiotic loading. At the 25 µg loading, the CRC-hydrogel, in Figure 12(b), showed more effective delivery with a larger inhibition zone (21 mm) compared to the CPC-hydrogel, in Figure 12(a), which produced an 18 mm zone. This difference is likely due to the CRC-hydrogel's superior swelling and porous network, which facilitated a more efficient antibiotic release. Interestingly, at the higher concentration of 50 µg, both hydrogels performed identically, producing a 25 mm zone, suggesting that at this loading, both hydrogels released enough amoxicillin to saturate the medium.

The results from the disk diffusion assay can be interpreted through the derived data regarding the diffusion rates of amoxicillin from the hydrogels. The inhibitory zones indicate the extent of antimicrobial activity, with larger zones suggesting more effective drug release. The diffusion of drug molecules within hydrogels is influenced by their physical structure, including porosity and swelling capacity [47]. The water-filled voids in the

hydrogels facilitate the movement of amoxicillin molecules from high to low concentration areas, demonstrating a Fickian diffusion process. Our findings show that the hydrogels displayed significant swelling, which not only increases porosity but also enhances the mobility of the entrapped amoxicillin, allowing for a more efficient release profile. Moreover, the observed results indicate that the entrapment of amoxicillin within cellulose-based hydrogels aids in its stabilization against degradation, allowing for tunable release profiles that can be modulated according to the hydrogel's physical properties. As illustrated by Wang et al. [48] sustained release is essential for counteracting antibiotic resistance by maintaining effective drug concentrations over extended periods.

4. CONCLUSIONS

To summarize, this research successfully demonstrates that cassava waste can be a valuable source for creating functional hydrogels with promising properties for drug delivery. Optimal conditions for starch removal were identified as 70 °C and 10 w/v%, which produced consistent cellulose from both cassava peel and cassava residue. The successful synthesis of these hydrogels was confirmed by FTIR analysis. The CRC-hydrogel proved to be structurally superior, with a highly porous network that resulted in better swelling and water retention. This advantage directly led to a higher entrapment efficiency and a faster, diffusion-controlled release of ascorbic acid. Furthermore, in an antibiotic delivery test, the CRC -hydrogel was more effective than the CPC-hydrogel at a 25 µg concentration of amoxicillin, though both performed identically at a higher concentration of 50 µg. The development opportunity between laboratory-scale synthesis and the performance of these hydrogels in pharmaceutical-grade applications is an issue for future investigation on kinetic-modelling; meanwhile, this research has shown promise for medicinal materials.

AUTHOR INFORMATION

Corresponding Author

Heri Satria — Department of Chemistry, Lampung University, Bandar Lampung-35141 (Indonesia);

orcid.org/0000-0003-0779-5830

Email: heri.satria@fmipa.unila.ac.id

Authors

Kamisah Delilawati Pandiangan — Department of Chemistry, Lampung University, Bandar Lampung-35141 (Indonesia);

orcid.org/0000-0001-6347-2361

Hapin Afriyani — Department of Chemistry, Lampung University, Bandar Lampung-35141

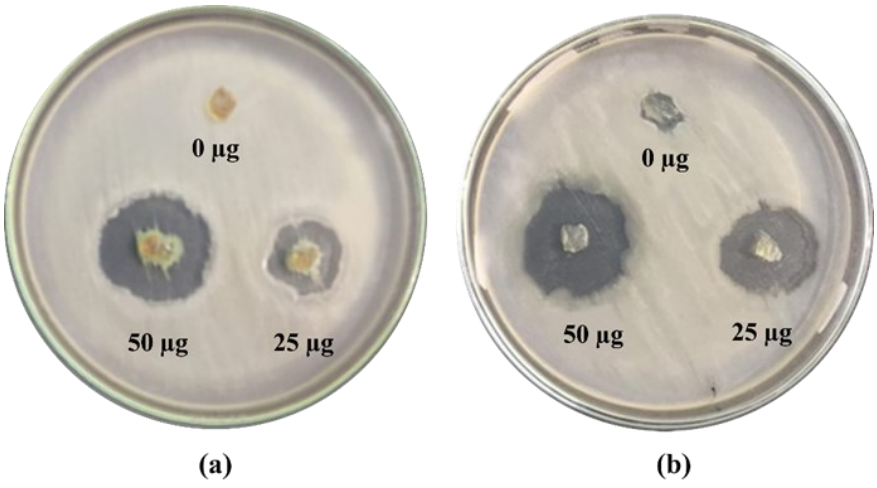

Figure 12. Kirby-Bauer disk diffusion assay results showing zones of inhibition for amoxicillin infused at various concentrations: (a) CPC-hydrogel and (b) CRC-hydrogel.

(Indonesia);
orcid.org/0000-0002-6092-127X
Diska Indah Alista — Department of Chemistry, Lampung University, Bandar Lampung-35141 (Indonesia);
orcid.org/0009-0002-1365-9704

Author Contributions

Conceptualization: H. S., K. D. P. and H. A.; Supervision, Methodology, Validation: H. S. and K. D. P.; Software, Data Curation, Visualization: H. S. and D. I. A.; Formal analysis, Writing - Original Draft: H. S., K. D. P., and D. I. A.; Writing - Review & Editing: H. S., K. D. P., H. A. and D. I. A.; Project administration: D. I. A.; Funding acquisition: H. S. Finally, all authors have read and agreed to the published version of the manuscript.

Conflicts of Interest

The authors have no conflicts of interest to disclose related to this publication.

ACKNOWLEDGEMENT

This study was conducted using the Research Innovation Collaboration project funding under contract number No:10614 /UN26/KS.00.00/2023 for Heri Satria, supported by the Higher Education Technology and Innovation (HETI) Project, University of Lampung.

DECLARATION OF GENERATIVE AI

The author(s) declare that no generative AI or AI -assisted technologies were used in the preparation of this manuscript.

REFERENCES

[1] U. K. Yaumidin, A. Priyanti, M. I. A. Irsyad, A. M. Hasibuan, D. O. Pribadi, H. Daulay, S. Aziz, E. Ariningsih, A. Zamroni, A. Ramadhan, D. Yuniati, and N. A. Ulya. (2026). "Harnessing Indonesia's Circular Bioeconomy: Integrating Land, Marine, Forest And Water Resources For Food System Sustainability". *Australian Journal of Agricultural and Resource Economics.* 10.1111/1467-8489.70088.

[2] N. Permatasari, S. Dali, and E. Wahyuni. (2023). "Potential Cassava Peel Waste (Manihot Esculenta Crantz) In The Production Of Bioethanol By Enzymatic Hydrolysis And Fermentation Using Zymomonas mobilis Bacteria". *The Journal of Pure and Applied Chemistry Research.* **12** (2): 87-103. 10.21776/ub.jpacr.2023.012.02.3304.

[3] F. Rachman, Y. Syahputri, and S. Sutanto. (2023). "Potential Of Cassava Peel As Cr Metal Biosorbent In Laboratory COD Waste". *Helium: Journal of Science and Applied Chemistry.* **3** (1): 21-28. 10.33751/helium.v3i1.7932.

[4] A. Olanbiwoninu and S. Odunfa. (2016). "Production Of Cellulase And Xylanase By Aspergillus terreus KJ829487 Using Cassava Peels As Substrates". *Advances in Microbiology.* **6** (7): 502-511. 10.4236/aim.2016.67050.

[5] P. M. Andrés, N. A. Rivera, I. M. Márquez, J. L. R. Arellano, G. I. B. López, and O. R. L. Ovalle. (2024). "Cassava Cultivation: Current And Potential Use Of Agroindustrial Co-Products". *AIMS Environmental Science.* **11** (2): 248-278. 10.3934/environsci.2024012.

[6] M. Budu, P. Boakye, and J. Bentil. (2025). "Scale-Up Of Tailor-Made Onsite Enzyme Blend From Cassava Peels For Industrial Bioethanol Production". *The Scientific World Journal.* **2025** (1): 1-10. 10.1155/tswj/2296078.

[7] A. Ma'ruf, E. Puspawiningtiyas, D. Afifah, and E. Díaz. (2023). "Synthesis And Characterization Of Cellulose Acetate Membrane From Cassava Peel For Microfiltration". *Nature Environment and Pollution Technology.* **22** (3): 1513-1518. 10.46488/nept.2023.v22i03.036.

[8] M. Adawiyah, D. Nuryansah, R. Suryani, and S. Hanifah. (2022). "The Effect Of Mass Ratio Mixture Of Durian Peel And Cassava Peel On The Quality Of Tissue Paper". *Journal of Physics: Conference Series.* **2190** (1): 1-8. 10.1088/1742-6596/2190/1/012025.

[9] S. Yuwono, E. Wahyuningsih, A. Kiswandono, W. Simanjuntak, and S. Hadi. (2021). "Characterization Of Carboxymethyl

Cellulose (CMC) Synthesized From Microcellulose Of Cassava Peel". *Materiale Plastice.* **57** (4): 225-235. 10.37358/mp.20.4.5422.

[10] A. Leite, C. Zanon, and F. Menegalli. (2017). "Isolation And Characterization Of Cellulose Nanofibers From Cassava Root Bagasse And Peelings". *Carbohydrate Polymers.* **157** : 962 -970. 10.1016/j.carbpol.2016.10.048.

[11] D. Hu, M. Zeng, Y. Sun, J. Yuan, and Y. Wei. (2021). "Cellulose-Based Hydrogels Regulated By Supramolecular Chemistry". *SusMat.* **1** : 266-284. 10.1002/sus2.17.

[12] H. Enawgaw, T. Tesfaye, K. T. Yilma, and D. Y. Limeneh. (2021). "Synthesis Of A Cellulose-Co-AMPS Hydrogel For Personal Hygiene Applications Using Cellulose Extracted From Corncobs". *Gels.* **7** (4): 1-10. 10.3390/gels7040236.

[13] M. O. Haque and M. I. H. Mondal. (2016). "Synthesis And Characterization Of Cellulose-Based Eco-Friendly Hydrogels". *Rajshahi University Journal of Science and Engineering.* **44** : 45-53. 10.3329/rujse.v44i0.30386.

[14] H. N. Abdelhamid and A. P. Mathew. (2022). "Cellulose-Based Nanomaterials Advance Biomedicine: A Review". *International Journal of Molecular Sciences.* **23** : 1-36. 10.3390/ijms23105405.

[15] Q. F. Guan, H. B. Yang, Z. M. Han, Z. C. Ling, C. H. Yin, K. P. Yang, Y. X. Zhao, and S. H. Yu. (2021). "Sustainable Cellulose-Nanofiber-Based Hydrogels". *ACS Nano.* **15** : 7889-7898. 10.1021/acsnano.1c01247.

[16] H. Jin, M. Kettunen, A. Laiho, H. Pynnönen, J. Paltakari, A. Marmur, O. Ikkala, and R. H. A. Ras. (2011). "Superhydrophobic And Superoleophobic Nanocellulose Aerogel Membranes As Bioinspired Cargo Carriers On Water And Oil". *Langmuir.* **27** (5): 1930-1934. 10.1021/la103877r.

[17] F. N. Kayati, C. W. Purnomo, Y. Kusumastuti, and Rochmadi. (2024). "Physical Properties Comparison Of Hydrogel From Cassava Starch Using Two Different Non-Toxic Crosslinkers". *Next Sustainability.* **4** : 100043. 10.1016/j.nxsust.2024.100043.

[18] W. Tanan, J. Panichpakdee, P. Suwanakood, and S. Saengsuwan. (2021). "Biodegradable Hydrogels Of Cassava Starch-g-Polyacrylic Acid Natural Rubber Polyvinyl Alcohol As Environmentally Friendly And Highly Efficient Coating Material For Slow-Release Urea Fertilizers". *Journal of Industrial and Engineering Chemistry.* **101** : 237-252. 10.1016/j.jiec.2021.06.008.

[19] K. Fang, Y. Zhang, J. Yin, T. Yang, K. Li, L. Wei, J. Li, and W. He. (2022). "Hydrogel Beads Based On Carboxymethyl Cassava Starch/Alginate Enriched With MgFe2O4 Nanoparticles For Controlling Drug Release". *International Journal of Biological Macromolecules.* **220** : 573-588. 10.1016/j.ijbiomac.2022.08.081.

[20] A. F. Chamorro, M. Palencia, and E. M. Combatt. (2024). "Biodegradable Cassava Starch/Phosphorite/Citric Acid Based Hydrogel For Slow Release Of Phosphorus: In Vitro Study". *Gels.* **10** (7): 1-16. 10.3390/gels10070431.

[21] A. Amanzholkyzy, S. Zhumagaliyeva, N. Sultanova, Z. Abilov, D. Ongalbek, E. Donbayeva, A. Niyazbekova, and Z. Mukazhanova. (2025). "Hydrogel Delivery Systems For Biological Active Substances: Properties And The Role Of HPMC As A Carrier". *Molecules.* **30** (6): 1-19. 10.3390/molecules30061354.

[22] V. Miljković, I. Savić, and L. Nikolić. (2021). "Waste Materials As A Resource For Production Of CMC Superabsorbent Hydrogel For Sustainable Agriculture". *Polymers.* **13** (23): 1-12. 10.3390/polym13234115.

[23] O. V. López, S. Z. Viña, A. N. A. Pachas, M. N. Sisterna, P. H. Rohatsch, A. Mugridge, H. E. Fassola, and M. A. García. (2010). "Composition And Food Properties Of Pachyrhizus Ahipa Roots And Starch". *International Journal of Food Science & Technology.* **45** (2): 223-233. 10.1111/j.1365-2621.2009.02125.x.

[24] Q. Ma, W. Zhou, X. Du, H. Huang, and Z. Gong. (2023). "Combined Dilute Sulfuric Acid And Tween 80 Pretreatment Of Corn Stover Significantly Improves The Enzyme

Digestibility: Synergistic Removal Of Hemicellulose And Lignin". *Bioresource Technology.* **382** : 129218. 10.1016/j.biortech.2023.129218.

[25] E. F. Okpalanma, E. S. Ukpong, C. C. Ezegbe, C. C. Nwagbo, and C. O. C. Chude. (2024). "Evaluation Of The Physico-Chemical Properties Of Cassava, Cocoyam, Sweet Potato Starches And Glucose Syrups Produced From The Hydrolysis Of The Starches With Sorghum Malt Enzyme Extract". *Food Science and Applied Biotechnology.* **7** (1): 24-35. 10.30721/fsab2024.v7.i1.314.

[26] C. Chatpapamon, D. Uttapap, Y. Wandee, C. Puttanlek, and V. Rungsardthong. (2021). "Glycerol-Enhancing Heat-Moisture Treatment Of A-Type Rice And Cassava Starches And B-Type Potato And Canna Starches". *International Journal of Food Science & Technology.* **56** (8): 4038-4049. 10.1111/ijfs.15027.

[27] R. Radakisnin, M. A. Majid, M. Ridzuan, M. Jawaid, M. T. H. Sultan, and M. F. M. Tahir. (2020). "Structural, Morphological And Thermal Properties Of Cellulose Nanofibers From Napier Fiber (Pennisetum purpureum)". *Materials.* **13** (18): 1-17. 10.3390/ma13184125.

[28] A. Hachaichi, B. Kouini, L. K. Kian, M. Asim, H. Fouad, M. Jawaid, and M. Sain. (2021). "Nanocrystalline Cellulose From Microcrystalline Cellulose Of Date Palm Fibers As A Promising Candidate For Bio-Nanocomposites: Isolation And Characterization". *Materials.* **14** (18): 1-12. 10.3390/ma14185313.

[29] A. V. T. Figueroa, C. J. P. Martinez, T. C. Castro, E. B. Martinez, M. A. G. C. Madueno, A. M. G. Alegria, T. E. L. Ceniceros, and L. A. Villegas. (2020). "Composite Hydrogel Of Poly(acrylamide) And Starch As Potential System For Controlled Release Of Amoxicillin And Inhibition Of Bacterial Growth". *Journal of Chemistry.* **2020** : 1-14. 10.1155/2020/5860487.

[30] L. Jiang, X. Huang, C. Tian, Y. Zhong, M. Yan, C. Miao, T. Wu, and X. Zhou. (2023). "Preparation And Characterization Of Porous Cellulose Acetate Nanofiber Hydrogels". *Gels.* **9** (6): 1-10. 10.3390/gels9060484.

[31] M. M. Al-Rajabi and Y. H. Teow. (2021). "Green Synthesis Of Thermo-Responsive Hydrogel From Oil Palm Empty Fruit Bunches Cellulose For Sustained Drug Delivery". *Polymers.* **13** (13): 1-21. 10.3390/polym13132153.

[32] B. C. Nguyen, T. Truong, N. T. Nguyen, D. N. Dinh, D. Hollmann, and M. N. Nguyen. (2024). "Advanced Cellulose-Based Hydrogel TiO2 Catalyst Composites For Efficient Photocatalytic Degradation Of Organic Dye Methylene Blue". *Scientific Reports.* **14** (1): 1-11. 10.1038/s41598-024-61724-w.

[33] P. Wei, W. Chen, Q. Song, Y. Wu, and X. You-Jia. (2021). "Superabsorbent Hydrogels Enhanced By Quaternized Tunicate Cellulose Nanocrystals With Adjustable Strength And Swelling Ratio". *Cellulose.* **28** (6): 3723-3732. 10.1007/s10570-021-03776-z.

[34] S. Zhou, K. Guo, D. Bukhvalov, X. F. Zhang, W. Zhu, J. Yao, and M. He. (2020). "Cellulose Hydrogels By Reversible Ion-Exchange As Flexible Pressure Sensors". *Advanced Materials Technologies.* **5** (9). 10.1002/admt.202000358.

[35] H. Shi, Y. Yang, Y. Huang, X. Li, and Y. Shi. (2023). "Anisotropic Single-Domain Hydrogel With Stimulus Response To Temperature And Ionic Strength". *Macromolecules.* **56** (2): 528-534. 10.1021/acs.macromol.2c01963.

[36] A. L. W. Jampi, S. F. Chin, M. E. Wasli, and C. H. Chia. (2021). "Preparation Of Cellulose Hydrogel From Sago Pith Waste As A Medium For Seed Germination". *Journal of Physical Science.* **32** (1): 13-26. 10.21315/jps2021.32.1.2.

[37] M. U. A. Khan, G. Stojanović, R. A. Rehman, A. Moradi, M. Rizwan, N. Ashammakhi, and A. Hasan. (2023). "Graphene Oxide-Functionalized Bacterial Cellulose-Gelatin Hydrogel With Curcumin Release And Kinetics: In Vitro Biological Evaluation". *ACS Omega.* **8** (43): 40024-40035. 10.1021/acsomega.2c06825.

[38] M. S. Ahmed, M. Maniruzzaman, M. R. Al-Mamun, M. A. Ali, M. M. R. Badal, M. A. Aziz, and M. Yousuf. (2023). "Jute Stick-Derived Cellulose-Based Hydrogel: Synthesis, Characterization, And Methylene Blue Removal From Aqueous Solution". *ACS Omega.* **8** (50): 47856-47873. 10.1021/acsomega.3c06349.

[39] W. H. W. Ishak, O. Y. Jia, and I. Ahmad. (2020). "pH-Responsive Gamma Irradiated Poly(Acrylic Acid)-Cellulose-Nanocrystal-Reinforced Hydrogels". *Polymers.* **12** (9): 1-14. 10.3390/polym12091932.

[40] L. Gao, H. Luo, Q. Wang, G. Hu, and Y. Xiong. (2021). "Synergistic Effect Of Hydrogen Bonds And Chemical Bonds To Construct A Starch-Based Water-Absorbing/Retaining Hydrogel Composite Reinforced With Cellulose And Poly(Ethylene Glycol)". *ACS Omega.* **6** (50): 35039-35049. 10.1021/acsomega.1c05614.

[41] Y. Xie, S. Gao, Z. Ling, C. Lai, Y. Huang, J. Wang, C. Wang, F. Chu, F. Xu, M. J. Dumont, and D. Zhang. (2022). "A Multiscale Biomimetic Strategy To Design Strong, Tough Hydrogels By Tuning The Self-Assembly Behavior Of Cellulose". *Journal of Materials Chemistry A.* **10** (26): 13685-13696. 10.1039/d2ta03262g.

[42] A. Ortega, S. Valencia, E. Rivera, T. Segura, and G. Burillo. (2023). "Reinforcement Of Acrylamide Hydrogels With Cellulose Nanocrystals Using Gamma Radiation For Antibiotic Drug Delivery". *Gels.* **9** (8): 1-16. 10.3390/gels9080602. 10.1021/acssuschemeng.0c08022

[43] M. Culebras, A. P. Barrett, M. Pishnamazi, G. Walker, and M. N. Collins. (2021). "Wood-Derived Hydrogels As A Platform For Drug-Release Systems". *ACS Sustainable Chemistry & Engineering.* **9** (6): 2515-2522. 10.1021/acssuschemeng.0c08022.

[44] M. U. A. Khan, S. I. A. Razaq, H. Mehboob, S. Rehman, W. S. Al-Arjan, and R. Amin. (2021). "Antibacterial And Hemocompatible pH-Responsive Hydrogel For Skin Wound Healing Application: In Vitro Drug Release". *Polymers.* **13** (21): 1-16. 10.3390/polym13213703.

[45] J. C. Q. Stéfano, V. A. Correa, S. D. H. Flores, and A. J. Alvarez. (2020). "pH-Sensitive Starch-Based Hydrogels: Synthesis And Effect Of Molecular Components On Drug Release Behavior". *Polymers.* **12** (9): 1-14. 10.3390/polym12091974.

[46] J. Claus, T. Eickner, N. Grabow, U. Kragl, and S. Oschatz. (2020). "Ion Exchange Controlled Drug Release From Polymerized Ionic Liquids". *Macromolecular Bioscience.* **20** (9): 2000152. 10.1002/mabi.202000152.

[47] N. Karakuş, S. Türk, G. G. Eskiler, M. Syzdykbayev, N. Appazov, and M. Özacar. (2024). "Investigation Of Tannic Acid Crosslinked PVA/PEI-Based Hydrogels As Potential Wound Dressings With Self-Healing And High Antibacterial Properties". *Gels.* **10** (11): 1-23. 10.3390/gels10110682.

[48] S. Wang, Z. Wang, C. Xu, L. Cui, G. Meng, S. Yang, J. Wu, Z. Liu, and X. Guo. (2021). "PEG-α-CD/AM/Liposome @Amoxicillin Double Network Hydrogel Wound Dressing—Multiple Barriers For Long-Term Drug Release". *Journal of Biomaterials Applications.* **35** (9): 1085-1095. 10.1177/0885328221991948.